MECH 576
Geometry in Mechanics

December 4, 2009

Kinematic Mapping and the Burmester Problem

1 Introduction

How many *precision positions* can a planar 4-bar mechanism be designed to fulfill? Given this number of specified poses of a Cartesian frame what are the dimensions and layout of mechanisms appropriate to the task? Answers to these questions constitute the Burmester problem (BP). An article by Chen *et al* [3] contains 23 pertinent references including the original Burmester treatment and four by Karl-Heinz Modler; TU-Dresden has been prominently involved, from the beginning. There are 9 items cited that pertain specifically to planar dyad or 4-bar design. The purpose of this introductory article is to detail the steps to be taken in formulating the problem in a general way and to expose a symbolic univariate polynomial solution along with the back substitutions necessary to uniquely define the remaining variables. Let us proceed with

- Representing a planar pose in *Blaschke-Grünwald* planar kinematic image space coordinates (BG),
- Transforming points, presented in the moving or end effector frame EE, to points in the fixed frame FF,
- Points that are bound to or move on circles in FF and
- Five given poses, four constraint equations and their reduction to a univariate quartic and the unique partner variables to each of the four.
- A *three* position problem example that is simpler, turning out to be linear, and possibly richer than the general five position problem because, given two fixed link centres, the designer has the freedom to move these to fit layout constraints that might arise in order to satisfy specific application requirements.

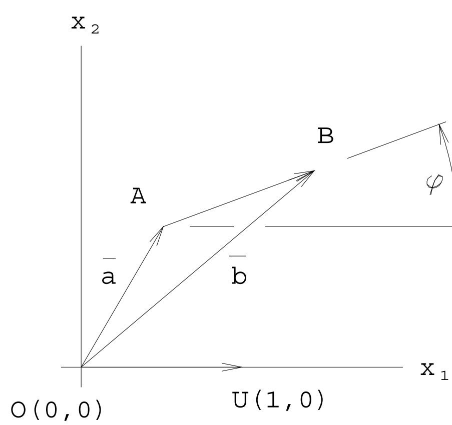

Figure 1: Pose Image

2 Pose to Image

Consider derivation of the BG of a planar displacement with respect to some "home" position or pose $\overrightarrow{OU}$, say, a unit vector on the origin pointing in the direction of positive x_1 where the Cartesian frame is Ox_1x_2. The given arbitrary finite displacement is the image $\overrightarrow{AB}$ of $\overrightarrow{OU}$. This is shown in Fig. 1 and the vectors **a** and **b** are the relative point displacement vectors. Note that φ is the positive, counterclockwise rotation angle of $\overrightarrow{AB}$ with respect to $\overrightarrow{OU}$.

$$\mathbf{a} = \begin{bmatrix} a_1 \\ a_2 \end{bmatrix}, \quad \mathbf{b} = \begin{bmatrix} b_1 \\ b_2 \end{bmatrix}$$

Half angles are always used in dual quaternion algebra. That way one need only consider full turns as half turns in either direction. Furthermore one may take $\sin\frac{\varphi}{2} \geq 0$, *i.e.*, $0 \rightarrow \pi$, only positive, counterclockwise rotations because with finite displacements one does not care whether the final position was achieved by turning one way rather than the other. In planar kinematic mapping this gives

$$c_0 = \cos\frac{\varphi}{2} = \pm\sqrt{\frac{1+\cos\varphi}{2}}, \quad c_3 = \sin\frac{\varphi}{2} = \pm\sqrt{\frac{1-\cos\varphi}{2}}, \quad \cos\varphi = \frac{b_1 - a_1}{|\sqrt{(b_1-a_1)^2 + (b_2-a_2)^2}|} \tag{1}$$

Homogeneous BG coordinates are defined as follows.

$$\{X_0 : X_1 : X_2 : X_3\} \equiv \{2c_0 : -d_2 : d_1 : 2c_3\}, \quad d_1 = a_1c_0 + a_2c_3, \quad d_2 = a_2c_0 - a_1c_3 \tag{2}$$

3 Point from EE to FF

To solve a BP one must find five variables p_1, p_2, m_1, m_2, R where $P(p_1, p_2)$ is a point in EE that must be constrained to lie on a circle κ with radius $\sqrt{R}$, centred on point $M(m_1, m_2)$ by transforming $P \rightarrow Q$ thus.

$$\begin{bmatrix} 1 \\ q_1 \\ q_2 \end{bmatrix} = \begin{bmatrix} 1 & 0 & 0 \\ 2(X_0X_2 + X_1X_3) & X_0^2 - X_3^2 & -2X_0X_3 \\ -2(X_0X_1 - X_2X_3) & 2X_0X_3 & X_0^2 - X_3^2 \end{bmatrix} \begin{bmatrix} 1 \\ p_1 \\ p_2 \end{bmatrix} \tag{3}$$

Derivation of the planar point transformation Eq. 3 is detailed in [5]. Normalizing the upper leftmost element as $4(X_0^2 + X_3^2) = 1$ makes this an equation rather than a proportionality that requires a multiplier. The circle equation in FF is

$$(q_1 - m_1)^2 + (q_2 - m_2)^2 - R = 0 \tag{4}$$

Five desired poses are given *a-priori*.

$$\left.\begin{matrix} V_i \\ W_i \\ X_i \\ Y_i \\ Z_i \end{matrix}\right\} \rightarrow X_i, \quad i = 1, 2, 3$$

Without loss in generality the first can be chosen as the home position $V\{1:0:0:0\}$.

4 Five Constraint Equations

The convention documented in Bottema and Roth's text [1] will be adopted. Their circle equation, our Eq. 4, augmented by the transformation Eq. 3, is reproduced here exactly, for reference.

$$\begin{aligned} C_0z^2(X_1^2 + X_2^2) + (C_1z - C_0x)zX_1X_3 \\ +(C_2z - C_0y)zX_2X_3 - (C_0y + C_2z)zX_1X_4 \end{aligned}$$

$$\begin{aligned} &+(C_0x + C_1z)zX_2X_4 + (C_2x - C_1y)zX_3X_4 \\ &+\frac{1}{4}[C_0(x^2+y^2) - 2C_1xz - 2C_2yz + C_3z^2]X_3^2 \\ &+\frac{1}{4}[C_0(x^2+y^2) + 2C_1xz + 2C_2yz + C_3z^2]X_4^2 = 0 \end{aligned} \tag{5}$$

Dehomogenizing and defining differences in notation with respect to those that were introduced above are detailed as follows.

- Set $X_0 \equiv X_4 = 1$.
- Set $z = 1$.
- Set $C_0 = 1$ if the constraint is a circle.
- Set $C_0 = 0$ if P moves on a line, *i.e.*, in the case of a slider.
- Only circle constraints are used in the formulation below.
- Note $C_1 = -m_1,\;\; C_2 = -m_2,\;\; C_3 = m_1^2 + m_2^2 - R$.

Thus Eq. 5 becomes, typically,

$$\begin{aligned} &(V_1^2+V_2^2) + (C_1 - p_1)V_1V_3 + (C_2 - p_2)V_2V_3 - (C_2+p_2)V_1 + (C_1+p_1)V_2 + (C_2p_1 - C_1p_2)V_3 \\ &+\frac{1}{4}(p_1^2+p_2^2 - 2C_1p_1 - 2C_2p_2 + C_3)V_3^2 + \frac{1}{4}(p_1^2+p_2^2+2C_1p_1+2C_2p_2+C_3) = 0 \end{aligned} \tag{6}$$

Using the simplification of V on the home position, the first constraint equation is written

$$p_1^2 + p_2^2 + 2C_1p_1 + 2C_2p_2 + C_3 = 0 \tag{7}$$

The second, for pose W, is written as Eq. 6 above but multiplied by $4/(W_3^2+1)$ to produce an interesting structure where p_1^2, p_2^2, C_3 appear isolated in the sum like they do in Eq. 7.

$$\begin{aligned} &p_1^2 + \frac{2(1-W_3^2)C_1p_1}{W_3^2+1} + \frac{4W_3C_2p_1}{W_3^2+1} + \frac{4(W_2 - W_1W_3)p_1}{W_3^2+1} + p_2^2 - \frac{4W_3C_1p_2}{W_3^2+1} + \frac{2(1-W_3^2)C_2p_2}{W_3^2+1} \\ &-\frac{4(W_1 - W_2W_3)p_2}{W_3^2+1} + \frac{4(W_2+W_1W_3)C_1}{W_3^2+1} + \frac{4(W_2W_3 - W_1)C_2}{W_3^2+1} + C_3 + \frac{4(W_1^2+W_2^2)}{W_3^2+1} \end{aligned} \tag{8}$$

Taking differences between Eq. 7 and the four equations, *i.e.*, Eq. 8 and its three partners written with X_i, Y_i, Z_i and multiplying the result by $(W_3^2+1)/4$, the inverse of the multiplier used to isolate p_1^2, p_2^2, C_3, produces Eq. 9 and its similar partners.

$$\begin{aligned} &W_1^2 + W_2^2 - W_3^2C_1p_1 - W_3^2C_2p_2 + W_3C_2p_1 - W_3C_1p_2 + (W_2 - W_1W_3)p_1 \\ &-(W_1 - W_2W_3)p_2 + (W_2 + W_1W_3)C_1 - (W_1 - W_2W_3)C_2 = 0 \end{aligned} \tag{9}$$

In the next step the bilinear terms C_1p_2, C_2p_1 are removed from the last three equations by taking differences of products with multipliers X_3, Y_3, Z_3 of Eq. 9 and remaining three with W_3. Using the first of the three equations devoid of terms C_1p_2, C_2p_1 in a similar manner, this time with multipliers

$$(X_3W_3^2 - W_3X_3^2) \quad \text{and} \quad (Y_3W_3^2 - W_3Y_3^2), (Z_3W_3^2 - W_3Z_3^2),$$

one obtains two linear equations. There are only four equations because there are really only *four* unknowns because R is defined explicitly by Eq. 7 and R was removed in the first subtraction. The set of four now looks like this.

$$\begin{aligned} a_0 + a_1p_1 + a_2p_2 + a_3C_1 + a_4C_2 + a_5p_1C_1 + a_5p_2C_2 + a_6p_1C_2 - a_6p_2C_1 &= 0 \\ b_0 + b_1p_1 + b_2p_2 + b_3C_1 + b_4C_2 + b_6p_1C_2 - b_6p_2C_1 &= 0 \\ c_0 + c_1p_1 + c_2p_2 + c_3C_1 + c_4C_2 &= 0 \\ d_0 + d_1p_1 + d_2p_2 + d_3C_1 + d_4C_2 &= 0 \end{aligned} \tag{10}$$

Do not confuse the compressed coefficients $c_{0,1,2,3,4}$ in Eq. 10 with the sines and cosines of $\varphi/2$ used in Eqs.1 and 2. In the next two steps, say, C_1 and C_2 can be eliminated to leave two quadrics in p_1 and p_2, *e.g.*,

$$A_{11}p_1^2 + A_{22}p_2^2 + A_{12}p_1p_2 + A_{00} = 0, \;\; B_{11}p_1^2 + B_{22}p_2^2 + B_{12}p_1p_2 + B_{00} = 0 \tag{11}$$

These two can be reduced to a *quartic* in either p_1 or p_2. Solving for the four values of p_1 –it has been shown that sometimes all four are real– and substituting them individually in 11

$$A_2p_2^2 + A_1p_2 + A_0 = 0, \;\; B_2p_2^2 + B_1p_2 + B_0 = 0 \tag{12}$$

yields Eqs. 12. These two can be solved for p_2 by eliminating p_2^2 so

$$(A_1B_2 - A_2B_1)p_2 - (A_2B_0 - A_0B_2) = 0 \tag{13}$$

C_1 and C_2 can of course be solved linearly with the last two of Eqs. 10.

5 A Three Position Problem

This problem is considered first because it may be somewhat easier to follow and relates the mapping exercise to two slightly different approaches to solutions obtained with geometric construction. Given data and solution to this problem are summarized in Fig. 2.

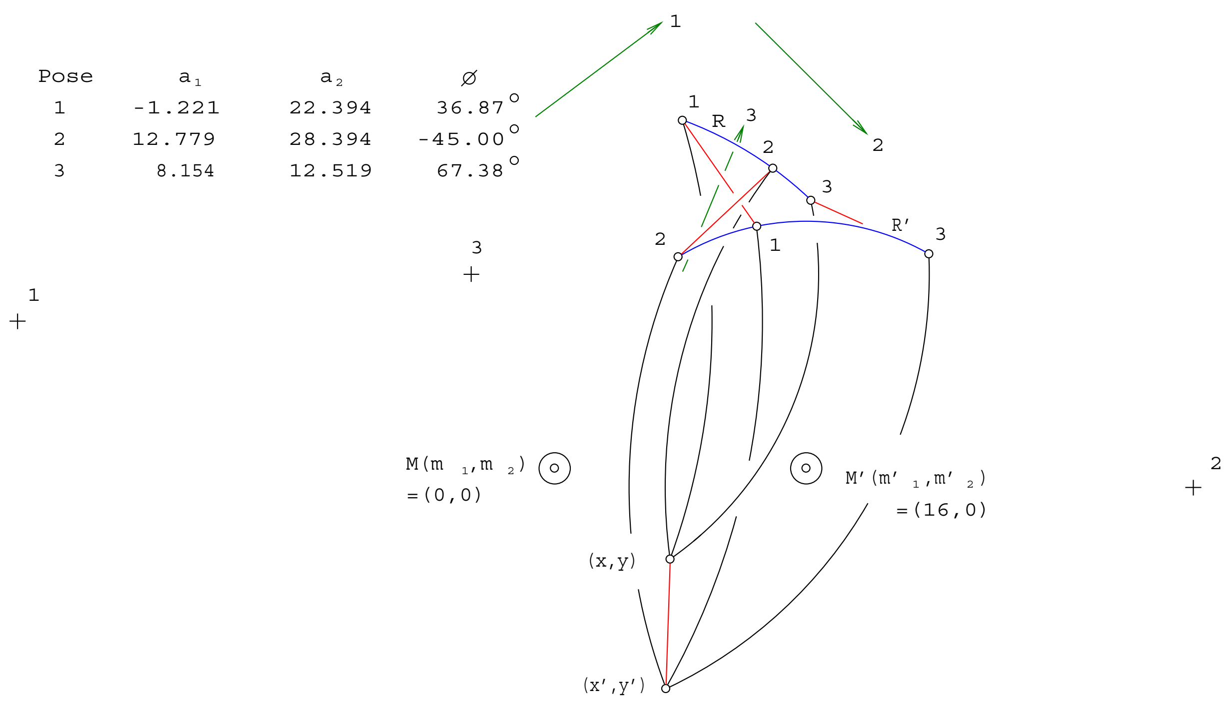

Figure 2: Design a Four Bar Mechanism Given Three EE Poses and Two Fixed Centres

The three given poses are represented by the arrows labeled $1, 2, 3$ and pertinent data is tabulated at upper left. (a_1, a_2) refers to the tail end point coordinates with respect to the given link centre on FF, $M(m_1, m_2) = (0, 0)$. Notice the second centre is located at $M'(m_1', m_2') = (16, 0)$. The task is to find the link lengths (squared) R, R' radiating from M, M' and the "home" positions $(x, y), (x', y')$ of the coupler end points that are displaced in three pair of concentric circular arc pairs about displacement pole centres marked $+1, +2, +3$. These arc pairs intersect the circles of radius $\sqrt{R}, \sqrt{R'}$ centred on M, M' to establish the three required coupler poses $11, 22, 33$ that correspond to the three given pose arrows $1, 2, 3$.

5.1 Three Constraint Equations

Eq. 5 becomes, after appropriate substitutions, Eq. 14.

$$
\begin{aligned}
X_{i1}^2 + X_{i2}^2 - (x+m_1)X_{i1}X_{i3} - (y+m_2)X_{i2}X_{i3} + (x-m_1)X_{i2} - (y-m_2)X_{i1} \\
-(m_2x - m_1y)X_{i3} + \frac{1}{4}[x^2+y^2+2(m_1x+m_2y)+m_1^2+m_2^2-R]X_{i3}^2 \\
+\frac{1}{4}[x^2+y^2-2(m_1x+m_2y)+m_1^2+m_2^2-R] = 0
\end{aligned} \tag{14}
$$

X_{ij} are computed with Eqs. 1 and 2 for each of the three EE poses using the given data. The three displacement pole locations are available immediately from Eq. 15, after dehomogenization with $X_0 = X_4 = 1$.

$$P_{+i}(p_{i1}, p_{i2}) = \left(\frac{X_{i1}}{X_{i3}}, \frac{X_{i2}}{X_{i3}}\right) \tag{15}$$

All this is summarized in the table below.

Pose	$X_0 = X_4$	X_1	X_2	X_3	p_{i1}	p_{i2}
1	1.8974	−21.6310	5.9229	0.6324	−34.2034	9.3654
2	1.8478	−31.1229	0.9403	−0.7654	40.6641	−1.2286
3	1.6641	−5.8934	13.7288	1.1094	−5.3123	12.3750

(16)

Three versions of Eq. 14, with available numerical values for each of three poses inserted, appear as Eq. 17. Note "home" position of pose arrow tail point x, y and radius squared R are the three unknowns.

$$
\begin{aligned}
503.9821 + 24.9180x + 37.2964y + x^2 + y^2 - R = 0 \\
969.5221 - 22.0829x + 58.2274y + x^2 + y^2 - R = 0 \\
223.2131 + 29.3843x - 5.4235y + x^2 + y^2 - R = 0
\end{aligned} \tag{17}
$$

Subtracting the first of Eq. 17 from the other two results in two linear equations in x, y, Eq. 18.

$$466.5400 - 47.0009x + 20.9310y = 0, \quad -279.7690 + 4.4664x - 42.7199y = 0 \tag{18}$$

Eliminate x between the first of Eq. 17 and Eq. 18 to yield an equation in y and R, Eq. 19, then eliminate x between both of Eq. 18 to get y. Get R with this value of y in Eq. 19. Square-rooting gets radius r.

$$1875.1862 + 126.4350y + 2.6472y^2 - 2.2091R = 0 \tag{19}$$

$$11.0657 + 1.9144y = 0 \rightarrow y = -5.7803, x = 7.35221, \quad 451.8090 - 0.8096R \rightarrow r = 23.6233$$

Repeating everything above, beginning with Eq. 17, but with $(m_1', m_2') = (16, 0)$ substituted into Eq. 14, produces x', y', R'.

$$25.1966 + 1.7967y' = 0 \rightarrow y' = -14.0236, x' = 7.0767, \quad 155.0005 - 0.6358R \rightarrow r = 15.7383$$

Notice that $\sqrt{(x-x')^2 + (y-y')^2} = 8.2479$. Referring back to Fig. 2, see how pairs of concentric arcs on the three poles swing the coupler, in its home position below, up to intersect the appropriate circles centred on M, M' so as to place the coupler in three required poses. To help visualize the situation, imagine that a large sheet of plywood is nailed to the coupler and an arrow is correctly painted on it so that when the four-bar mechanism is moved the painted arrows will match the ones specified in the course of the coupler's trajectory. As an exercise, compute **a** and φ, as shown on Fig. 1, where A is the tail of the arrow and the home position of the coupler is represented by $\overrightarrow{OU}$ with O at the end given by x, y.

5.2 A Constructive Solution

Recall that the Burmester problem is not about 4-bar mechanisms *per-se* but about 2R dyads. Therefore what follows pertains only to the dyad peculiar to given point $M(0,0)\odot$ and the three given pose arrows that represent planar Cartesian EE frames. The construction shown in Fig. 3 would have to be repeated for $M'(16,0)$ the other given R-joint in FF in order to produce a second dyad to complete the 4-bar. The sequence of geometric constructions in Fig. 3 shows how the problem can be solved without numerical computation. It also illustrates an application of both kinematic inversion and the displacement pole. Note that a constructive solution implies an algebraic solution of degree 2 or 1 and this agrees with the set of linear equations, Eqs. 18 and 19, formulated in the mapping exercise.

5.2.1 Inversion

The three constructions in the top row of Fig. 3 locate three points on the circle traced by the R-joint that joins the two rigid body links of the dyad. The first drawing, on the left, locates point 1 by assuming that M and arrow 1 are in proper relationship and arrows 2 and 3 are displaced to coincide with arrow 1 while moving M as if it were on a rigid body with the arrows, which it is. This implies a rotation about the R-joint centre 1, as yet unlocated. The displacements of M are marked with $\bigcirc$. Clearly these together with $\odot$ are on a circle centred on the desired point 1. The top centre and right hand drawings do the same to locate points 2 and 3 by, respectively, assuming that arrows 2 and 3 are in fixed juxtaposition with M and rotations are executed about R-joint centres at 2 and 3, respectively.

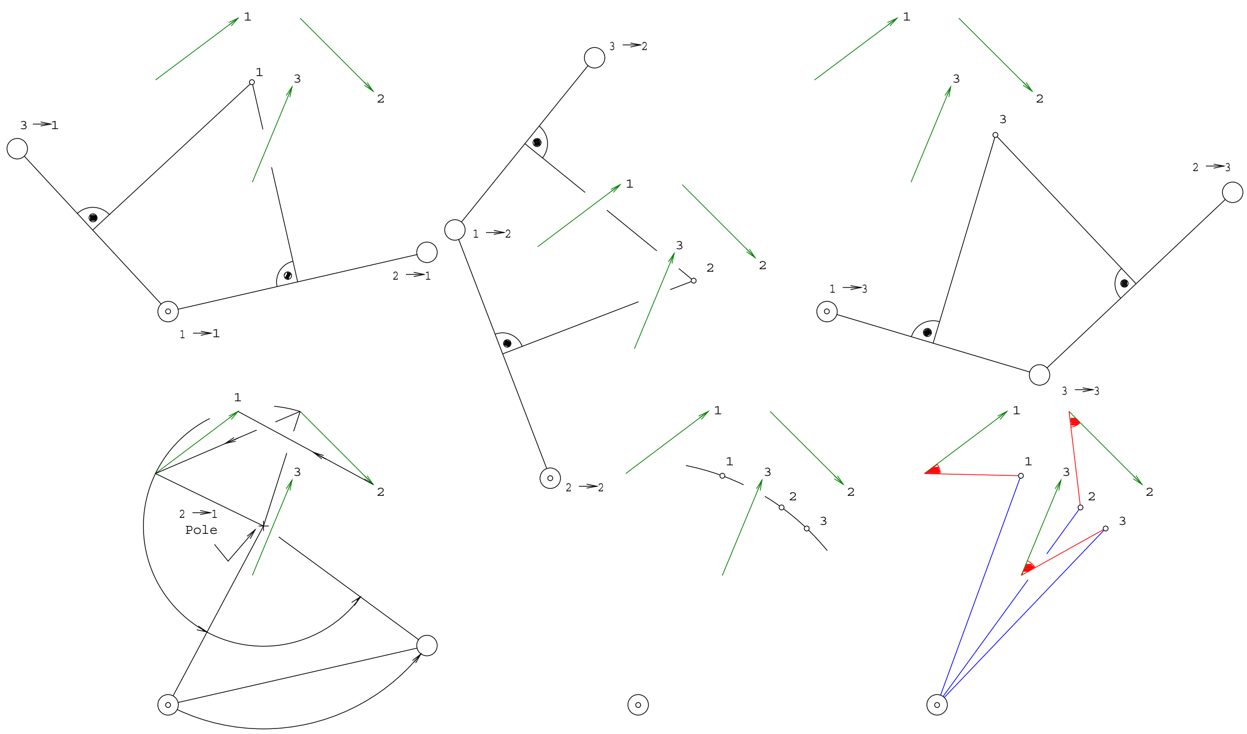

Figure 3: Solution by Geometric Constuction

5.2.2 Pole

The lower left drawing illustrates one of the two displacements of pose arrows and M depicted at upper left. It is the one labeled $2 \rightarrow 1$ there. Notice that the displacement pole is found at the intersection of right bisectors of the two vectors that translate the tip of arrow 2 to the tip of arrow 1 and, similarly, the respective tails. After finding the polar angular rotation magnitudes necessary to do this $\odot$ is rotated through the same angle about the pole to position $\bigcirc$ shown in the lower left drawing. The difference between what was done at upper left, as opposed to lower left, is that the former is essentially a "cut-and-paste" operation to obtain two chords that are right bisected to get point 1 while the latter shows a polar rotation that produces the other end of one of these chords.

5.2.3 Results

The lower middle and right hand drawings show the R-joint centre circle's arc of travel in assuming the three given poses and lines representing the two dyad rigid body links. Notice the line segment joining the R-joint centre to the pose arrow tail is the same length and makes the same angle at the tail vertex at all three poses. This verifies the solution.

6 A Five Pose Example

To begin with, as in the three pose example, the kinematic image space coordinates are calculated and shown in 20 using data given in Fig. 4, similar to the tabulation 16. However the "home" position or pre-images (x, y) of points bound to move on circles traced the end points of links revolving about fixed points are unknowns this time.

Pose	$X_0 = X_4$	X_1	X_2	X_3
1	2.0000	0.0000	0.0000	0.0000
2	1.9982	-1.7897	-1.9054	0.0841
3	1.9930	-3.5071	-6.7758	0.1670
4	1.9923	-2.7530	-9.9252	0.1750
5	1.9941	-1.6213	-11.2817	0.1540

(20)

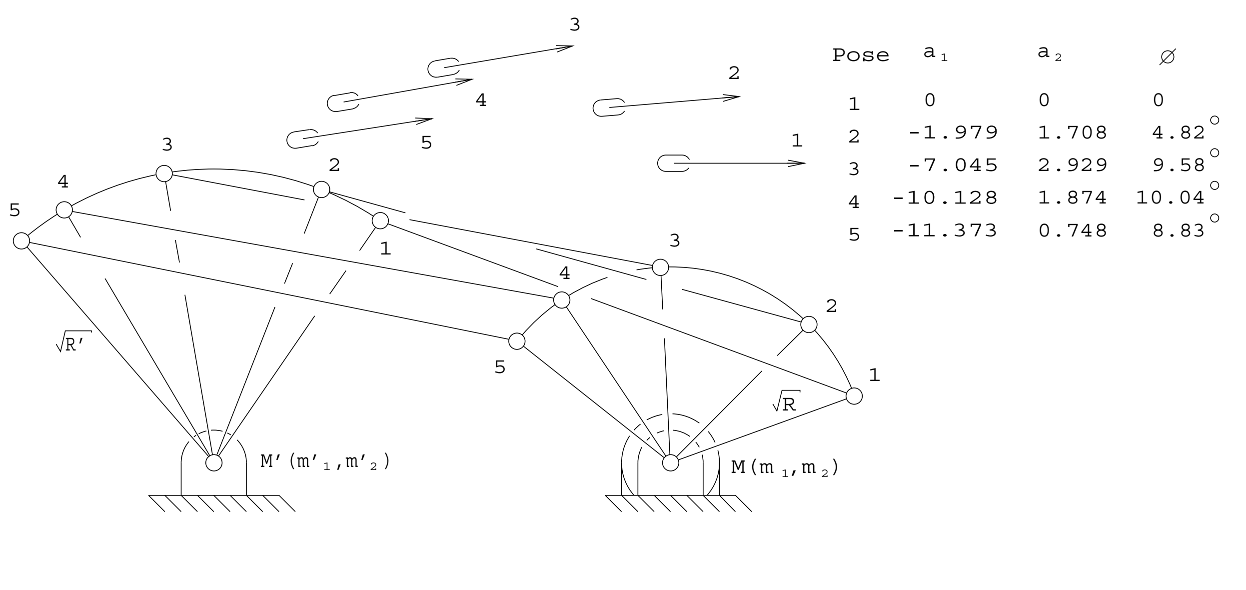

Figure 4: A Four-Bar Mechanism and Five Given Poses that It Can Achieve

In the following calculation $X_0 \equiv X_4 \neq 0$, with values as tabulated in 20, have been used in five versions of Eq. 5 having set $C_0 = 1$ and $z = 1$. These five constraint equations appear as

$$
\begin{aligned}
x^2+y^2+C_3+2C_1x+2C_2y=0\\
x^2+y^2+C_3+1.9929(C_1x+C_2y)+0.1681(C_2x-C_1y)\\
-3.958C_1+3.416C_2-3.657x+3.7365y+6.8337=0\\
x^2+y^2+C_3+1.9721(C_1x+C_2y)+0.3328(C_2x-C_1y)\\
-14.09C_1+5.858C_2-12.9186x+8.1212y+58.2111=0\\
x^2+y^2+C_3+1.9694(C_1x+C_2y)+0.3487(C_2x-C_1y)\\
-20.256C_1+3.748C_2-19.2924x+7.2219y+106.0883=0\\
x^2+y^2+C_3+1.9763(C_1x+C_2y)+0.307(C_2x-C_1y)\\
-22.746C_1+1.496C_2-22.2468x+4.9699y+129.9046=0
\end{aligned}
\tag{21}
$$

Retaining the first of Eq. 21 and subtracting it from the other four, after coefficient cross-multiplication, removes $x^2+y^2+C_3$ from them.

$$
\begin{aligned}
-0.007073(C_1x+C_2y)+0.1681(C_2x-C_1y)-3.958C_1+3.416C_2-3.657x+3.7365y+6.8337=0\\
-0.02789(C_1x+C_2y)+0.3328(C_2x-C_1y)-14.09C_1+5.858C_2-12.9186x+8.1212y+58.2111=0\\
-0.03063(C_1x+C_2y)+0.3487(C_2x-C_1y)-20.256C_1+3.748C_2-19.2924x+7.2219y+106.0883=0\\
-0.0237(C_1x+C_2y)+0.307(C_2x-C_1y)-22.746C_1+1.496C_2-22.2468x+4.9699y+129.9046=0
\end{aligned}
\tag{22}
$$

In the next step, retaining the first of Eq. 22, the term C_1x+C_2y is removed from the remaining ones as shown in Eq. 23.

$$
\begin{aligned}
-0.002333(C_2x-C_2y)+0.01074C_1-0.05385C_2+0.01063x-0.04678y+0.2211=0\\
-0.002681(C_2x-C_1y)-0.02204C_1-0.07811C_2-0.02445x-0.06336y+0.541=0\\
-0.001812(C_2x-C_1y)-0.06706C_1-0.07039C_2-0.07066x-0.05342y+0.7568=0
\end{aligned}
\tag{23}
$$

In the final stage, retaining the first of Eq. 23, the term C_2x-C_1y has been removed from the others leaving two linear equations, Eq. 24.

$$
0.8022C_1+0.3789C_2+0.8553x+0.2242y-6.695=0,\quad 1.7591C_1+0.6666C_2+1.8412x+0.3986y-13.65=0 \tag{24}
$$

Now the system of the first of Eqs. 22 and 23 and both of Eqs. 24 can be immediately reduced to the pair of conics, Eq. 25, by using the linear equations to eliminate C_1, C_2.

$$
\begin{aligned}
294.6811+15.6451x+19.5161y-2.4393x^2+4.6842xy+0.144y^2=0\\
348.1528+23.6499x+45.2113y-1.4153x^2+3.4524xy+0.3035y^2=0
\end{aligned}
\tag{25}
$$

The quartic resultant in x between Eqs. 25 is Eq. 26 and the four roots, in this case, are all real. Eliminating a variable, via Bezout's method, between a pair of conics is explained in [6] however mathematical software packages perform this step automatically with built-in *resultant* algorithms.

$$
\begin{aligned}
538.4046-614.6815x+21.7583x^2+12.6424x^3+0.1945x^4=0 \qquad (26)\\
x_1=0.9224,\quad x_2=5.3885,\quad x_3=-8.9276,\quad x_4=-62.3859
\end{aligned}
$$

To get the corresponding four values of y one may eliminate y^2 between Eqs. 25 and use Eq. 27 with the four values of x, above.

$$
\begin{aligned}
39.3021+1.3425x-0.5881y-0.5366x^2+0.9246xy=0 \qquad (27)\\
y_1=-151.4112,\quad y_2=-7.0448,\quad y_3=-1.7473,\quad y_4=-36.603
\end{aligned}
$$

Corresponding values of fixed link circle centres $C_1 = -m_1$ and $C_2 = -m_2$ are obtained, linearly, with Eq. 25 and their radius r from C_3 with the first of Eq. 21. The values of x and y are repeated here, too.

Sequence	x	y	C_1	C_2	C_3	r
1	0.9224	−151.4112	6.3607	91.6985	4830.4261	60.1552
2	5.3885	−7.0448	0.2562	9.1311	47.2266	6.0179
3	−8.9276	−1.7473	14.0396	9.1318	199.8370	8.9813
4	−62.3859	−36.6030	66.1837	40.0295	5956.4820	5.1151

(28)

6.1 Summing Up

6.1.1 Coupler Length

What is provided by the tabulation 28 is not exactly a design for a 4-bar mechanism, where EE the rigid body attached to its coupler can assume the five given planar poses, but, in this case, four *real* RR dyads whose second link, not attached to FF, becomes EE. Any of six pairs of dyads can be configured as a more or less appropriate mechanism. The coupler length L is immediately available by obtaining the distance between the two "home" point positions, one on each dyad's EE, that, under polar displacement, will lie on its respective crank circle. This distance, choosing the second and third dyads tabulated in 28, is just

$$L = \sqrt{(x_2 - x_3)^2 + (y_2 - y_3)^2} = \|\sqrt{(5.3885 + 8.9276)^2 + (-7.0448 + 1.7473)^2}\| = 15.2645$$

6.1.2 An Exercise

Review the displacement pole calculation procedure described by Eq. 15. Calculate the poles, for the two dyads selected above, for each of the five given poses. Do the arc intersection procedure illustrated in Fig. 2 to find the required crank angles for the 4-bar. The constructed arcs will contain the respective "home" position (x,y) and intersect the appropriate crank circle. What should one do about the fact that, in general, each polar displacement arc will intersect its respective crank circle *twice*?

6.1.3 Imprecision

The problem formulated in Fig. 4 was constructed *a-priori* to be free of singularity transgression, unlike the previous three position problem where poses and anchor points were chosen more or less arbitrarily. Furthermore some of the 5-pose 4-bar design and output parameter were selected. These, and those that have been calculated so far are tabulated in 29. Subscripts $_R$ and $_L$ refer to the right and left dyads of the 4-bar in Fig. 4. Crank angles $\theta_{R,L}$ are measured anticlockwise from 3-o'clock.

Parameter	Designed	Calculated
$M_R(x, y)$	$(-0.106, -9.176)$	$(-0.2563, -9.1311)$
$M_L(x, y)$	$(-14.106, -9.176)$	$(-14.0396, -9.1318)$
r_R	6	6.0179
r_L	9	8.9813
L	15.5	15.2648
$(\theta_R, \theta_L)_1$	$(19.92, 55.47)^\circ$	exercise
$(\theta_R, \theta_L)_2$	$(45.00, 68.47)^\circ$	exercise
$(\theta_R, \theta_L)_3$	$(92.83, 99.76)^\circ$	exercise
$(\theta_R, \theta_L)_4$	$(123.69, 120.60)^\circ$	exercise
$(\theta_R, \theta_L)_5$	$(141.60, 130.93)^\circ$	exercise

(29)

It is uncertain whether the discrepancies between measured and calculated results in the 5-pose problem are due to a) truncation of input data at two decimal places, b) round-off error due to successive subtraction of numbers of similar magnitude, c) poses that deviate within a narrow range of orientation, d) human input transcription error buried in the code and still undetected or e) yet some other undetermined oversight.

7 Conclusion

- The article [4] is recommended to those who wish to try the exercise suggested above because the coupler length/crank angle computations are carried out in detail therein.
- For more in-depth treatment of four-bar mechanism synthesis readers are referred to work by Brunnthaler *et al* [2]. However engineers may be reluctant to add the complication of more theory before sorting out problems of reliable design calculation already evident in the two relatively elementary exercises treated here.
- Another argument, in addition to design freedom, in favour of the 3-pose problem solution being a more effective engineering tool than the 5-position problem is that three approaches have been applied to the former and demonstrated to produce results that match closely, unlike the 1 to 2% discrepancies evident in the constructed -*vs*- computed 5-pose example.
- Observe that the short arcs of the circles centred on M, M', respectively, contain $1, 2, 3$ and $2, 1, 3$ in respective clockwise sequence in the 3-pose problem. That means the mechanism must pass through singularity in the course of its assigned task. This can be accomplished either by driving *both* fixed R-joints or using some sort of trip-and-reset mechanism to bias the return motion when passing the singularity. Consider that in the 5-pose problem a design, however compact and otherwise attractive, is more highly prone to poses being separated by a singularity cross-over. This issue is discussed at some length in [7].

Acknowledgement This set of notes was inspired by demonstration, by Guido Lonij at RWTH-Aachen in November 2008 using "Cinderella" software, of a constructive solution to the three position problem, done in three ways in section **5**. After having forgotten what he was shown the frustrated author embarked upon this rather lengthy re-investigation.

References

[1] Bottema, O. and Roth, B. (1990) *Theoretical Kinematics*, Dover.

[2] Brunnthaler, K., Pfurner, M. and Husty, M. (2006) "Synthesis of Planar Four-Bar Mechanisms", *Trans. Can. Soc. Mech. Eng.*, v.30, n.2, pp.297-313.

[3] Chen, C., Bai, S. and Angeles, J. (2007) "A Comprehensive Solution of the Classic Burmester Problem", *Trans. Can. Soc. Mech. Eng.*, v.32, n.2, pp.137-154.

[4] Hayes, M.J.D. and Zsombor-Murray, P.J. (2002) "Solving the Burmester Problem Using Kinematic mapping", *Proc. ASME-DETC2002*, MECH-34378, Montréal, 02-09.

[5] Zsombor-Murray, P.J. (2009) "Planar Kinematic Mapping Fundamentals", <http://cim.mcgill.ca/~paul/PKMF6Ac.pdf>, 7pp.

[6] Zsombor-Murray, P.J. (2009) "Solving Simultaneous Multivariate Polynomial Equations", <http://cim.mcgill.ca/~paul/CuQBM.pdf>, 10pp.

[7] Zsombor-Murray, P.J. (2009)"Two Degree of freedom Planar Parallel Manipulators and the Burmester Problem", <http://cim.mcgill.ca/~paul/IFToMM6aw.pdf>, 10pp.